



ON THE APPLICABILITY OF POST-IR IRSL DATING TO JAPANESE LOESS

CHRISTINE THIEL^{1,2}, JAN-PIETER BUYLAERT^{2,3}, ANDREW S. MURRAY² and SUMIKO TSUKAMOTO¹

¹*Leibniz Institute for Applied Geophysics, S3: Geochronology and Isotope Hydrology, Stilleweg 2, 30655 Hannover, Germany*

²*Nordic Laboratory for Luminescence Dating, Department of Earth Sciences, Aarhus University,
Risø DTU, DK 4000 Roskilde, Denmark*

³*Radiation Research Division, National Laboratory for Sustainable Energy, Risø DTU, DK 4000 Roskilde, Denmark*

Received 15 June 2010

Accepted 19 April 2011

Abstract: Recent work on infrared stimulated luminescence (IRSL) dating has focussed on finding and testing signals which show less or negligible fading. IRSL signals measured at elevated temperature following IR stimulation at 50°C (post-IR IRSL) have been shown to be much more stable than the low temperature IRSL signal and seem to have considerable potential for dating. For Early Pleistocene samples of both European and Chinese loess natural post-IR IRSL signals lying in the saturation region of the laboratory dose response curve have been observed; this suggests that there is no significant fading in nature. As a contribution to the further testing of post-IR IRSL dating, we have used 18 samples from two Japanese loess profiles for which quartz OSL and tephra ages up to 600 ka provide age control. After a preheat of 320°C (60 s), the polymimetal fine grains (4-11 µm) were bleached with IR at 50°C (200 s) and the IRSL was subsequently measured at 290°C for 200 s. In general, the fading uncorrected post-IR IRSL ages agree with both the quartz OSL and the tephra ages. We conclude that the post-IR IRSL signal from these samples does not fade significantly and allows precise and accurate age determinations on these sediments.

Keywords: post-IR IRSL dating, fading, Japanese loess.

1. INTRODUCTION

Feldspar has considerable potential for extending the age range of luminescence dating because the infrared stimulated luminescence (IRSL) signals from feldspar have a much higher characteristic saturation dose (so called D_0 value; $2*D_0 \sim 1\text{-}1.5$ kGy), compared to the optically stimulated luminescence (OSL) signal from quartz (where $2*D_0$ is typically ~ 0.20 kGy). However, feldspar suffers from anomalous fading, i.e. a decrease of the IRSL signal with time faster than expected from thermal stability measurements (Wintle, 1973; Spooner, 1994). This usually results in considerable age underestimations.

The models proposed to correct for the age underestimation (Lamothe and Auclair, 1999; Huntley and Lamothe, 2001) are strictly only applicable to the linear part of the dose response curve, i.e. to young samples (<50 ka). Lamothe *et al.* (2003) and Kars *et al.* (2008) have since proposed approaches which purport to allow for correction beyond the linear part of the dose response curve and thus can in principle be used for older material. However, all corrections models involve un-testable assumptions, including that the fading rate observed on a laboratory timescale is relevant to geological time (e.g. Huntley and Lamothe, 2001; Morthekai *et al.*, 2008).

Recent developments in luminescence dating offer the potential to circumvent the problem of anomalous fading. Thomsen *et al.* (2008) observed that a post-IR IRSL sig-

Corresponding author: C. Thiel
e-mail: christine.thiel@liag-hannover.de

nal (IR stimulation at 50°C and subsequent IRSL measurement at 225°C, blue detection) faded more slowly than conventional IRSL measured at a low stimulation temperature (usually 50°C, blue detection). The potential of post-IR IRSL dating (preheat of 250°C for 60 s and post-IR IR stimulation at 225°C for 100 s) of sand-sized potassium feldspar has successfully been tested by Buylaert *et al.* (2009); the fading rate could be reduced by a factor of two compared to the conventional IRSL measurements at 50°C. Based on the findings of Murray *et al.* (2009) that the dosimetry trap is not significantly eroded by preheating up to 320°C, Thiel *et al.* (2011) adopted a more stringent preheat of 320°C for 60 s, which allowed for post-IR IR stimulation at significantly higher temperatures. Because it is advisable to keep the stimulation temperature sufficiently below the preheat temperature to avoid a TL contribution contaminating the optically stimulated signal, Thiel *et al.* (2011) chose to investigate the use of post-IR IR stimulation at 290°C. Following the trend observed by Thomsen *et al.* (2008), it was expected that the measured fading rate is even smaller than for the stimulation temperature tested by Buylaert *et al.* (2009), because the higher stimulation temperature should allow charge in more distant trap/recombination centres to recombine. Most interestingly, Thiel *et al.* (2011) found the natural signal of a sample from below the Brunhes/Matuyama (B/M) boundary (~780 ka, expected natural dose >2700 Gy) in saturation on the laboratory regenerated dose response curve, which implies that there is no evidence for anomalous fading in the field using post-IR IR stimulation at 290°C. Therefore, even though a small fading rate of ~1%/decade was measured, the fading-uncorrected post-IR IRSL ages were considered to be the most reliable of all the ages presented (Thiel *et al.*, 2011). However, this study was hampered by the quality of the independent age control; only one post-IR IRSL age could be compared with a cluster of radiocarbon ages derived from charcoal.

Whereas independent age control, especially beyond the datable age range of radiocarbon, is lacking in most European loess sequences (e.g. Frechen *et al.*, 1997; Novothny *et al.*, 2002, Thiel *et al.*, 2011), Japanese deposits often include marker tephras for which ages are available (e.g. Machida and Arai, 2003). Watanuki *et al.* (2005) presented a detailed study on quartz and feldspar luminescence dating of two loess sites in Japan, which could be compared with tephra ages up to 600 ka. Using the same set of samples as Watanuki *et al.* (2005) we test the applicability of the single aliquot regenerative (SAR) dose post-IR IRSL measurement protocol (preheat: 320°C for 60 s, post-IR IR stimulation at 290°C) for dating polymineral fine grains (4–11 µm) extracted from the loess. All standard laboratory tests such as recuperation, recycling ratios and the ability of this protocol to measure a known dose given in the laboratory are presented and discussed. Laboratory fading rates are also determined and for both sites the derived ages (corrected

and uncorrected) are compared with the quartz OSL and tephra ages presented in Watanuki *et al.* (2005).

2. SAMPLING LOCATIONS AND INDEPENDENT AGE CONTROL

In the study of Watanuki *et al.* (2005) two sequences composed of loessic material intercalated with several tephra were investigated (**Fig. 1**). A short description of the samples and age control is given below.

At Tsunan-cho in the Niigata Prefecture (**Fig. 1a**), Central Japan, an up to 9 m thick sequence covering the oldest terrace (Taniage terrace) was sampled (Watanuki *et al.*, 2005; **Fig. 1b**). The Aira-Tanzawa (AT) tephra was found at a depth of 0.4 m below top ground surface (Hayatsu and Arai, 1981). Machida and Arai (2003) presented an age of 26–29 ka for this tephra, based on the correlation of $\delta^{18}\text{O}$ data derived from deep sea cores and the position of AT. Miyairi *et al.* (2004) presented an uncalibrated high precision radiocarbon age of $25,120 \pm 270$ BP for this tephra. One metre further down the section, the Daisen Kurayoshi Pumice (DKP; ~55 ka or older; Machida and Arai, 2003) could be identified. The tephra recognised at a depth of 2.8 m below top ground surface was referred to as the Iizuna-Kamitaru tephra (Iz-KT tephra; 125–150 ka; Suzuki, 2001) because of its position between the Aiyoshi scoria (b) (AY (b); 2.6 m below surface) and the Honokisaka scoria (HK; 3.3 m below surface); for the latter two no ages are available. Watanuki *et al.* (2005) assumed that a tephra of the APm tephra group lies about 9 m below top ground surface in the section, because this tephra was found by Hayatsu and Arai (1981) at this depth at a location nearby and equivalent to the outcrop of Watanuki *et al.* (2005). In a later study, the oldest from this tephra group (A1Pm) from the source area was dated to 388 ± 25 ka using red isothermal thermoluminescence (RITL; Tsukamoto *et al.*, 2007).

From the Niigata section, ten of the twelve samples presented in Watanuki *et al.* (2005) were used. Information on the samples and intercalated tephras is listed in **Table 1**.

At Ogawa-machi in the Tochigi Prefecture (**Fig. 1a**) loessic sediments deposited on the Kitsuregawa Hill and surrounding hill slopes were sampled. **Fig. 1c** shows a simplified sequence which originates from individual outcrops, i.e. indicated depths are not to be correlated with original sampling depths. The interbedded tephras were dated by means of fission track and radiocarbon dating (Kaizuka *et al.*, 2000; Suzuki *et al.*, 1998; Suzuki, 2001; Machida and Arai, 2003). The Akagi Kanuma Pumice (Ag-KP; 45 ka or older) was identified, followed by the Aso-4 tephra (85–90 ka), the Iizuna-Kamitaru tephra (Iz-KT; 125–150 ka) and the APm-U tephra (130 ± 30 ka). Furthermore, the Kurodahara tephra (KdP; 200 ± 30) and Nemoto-13, -14 and -16 (Nm-13, -14, -16; 330 ± 400 ka) were found (Watanuki *et al.*, 2005); Nm-16

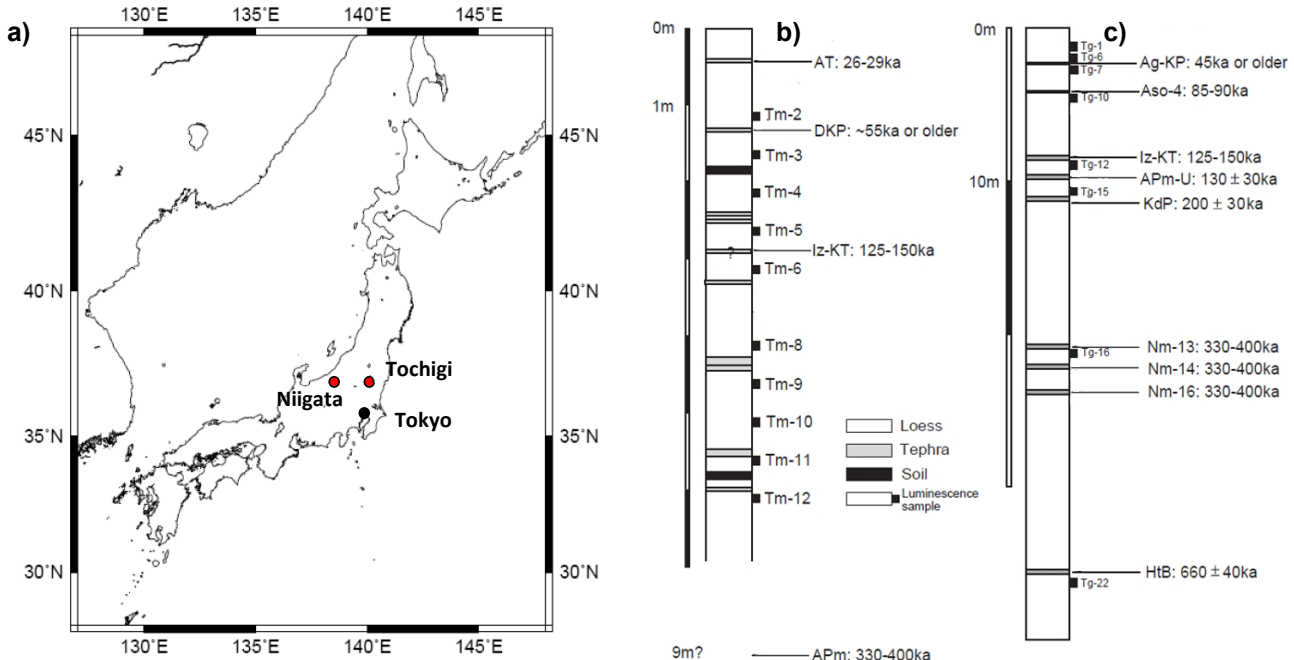


Fig. 1. a) Sampling locations; b) loess section at Tsunan-cho in Niigata Prefecture, Central Japan; c) loess section at Ogawa-machi in Tochigi Prefecture, Eastern Japan. Redrawn from Watanuki *et al.*, 2005.

is equivalent to A1Pm, dated to 388 ± 25 ka (Tsukamoto *et al.*, 2007). In addition the Hoshitoge Biotite tephra (HtB; 660 ± 40 ka) was excavated in the sequence.

From the Tochigi section eight of the twelve samples presented in Watanuki *et al.* (2005) were used. Information on the samples and intercalated tephras is listed in **Table 1**.

3. POST-IR IRSL MEASUREMENTS

Sample preparation and dosimetry measurements are described in detail in Watanuki *et al.* (2005). Equivalent dose (D_e) measurements were made with an automated Risø TL/OSL reader (DA-20; Thomsen *et al.*, 2006) using a calibrated $^{90}\text{Sr}/^{90}\text{Y}$ beta source (~ 0.21 Gy/s). The feldspar signal of the polymineral fine grains ($4\text{--}11\ \mu\text{m}$), mounted on aluminium discs, was stimulated with infrared light diodes emitting at 870 nm, and the luminescence was detected in the blue-violet region through a Schott BG39/Corning 7-59 filter combination. A SAR protocol was used to measure the equivalent dose (one aliquot run at a time). After a preheat of 320°C for 60 s the polymineral fine grains were bleached with IR diodes at 50°C for 200 s and subsequently stimulated with IR diodes for another 200 s but now with the sample held at 290°C . It is the latter IRSL signal that is used in the calculations, and we refer to this post-IR IRSL as pIRIR₂₉₀. The response to a test dose was measured in the same manner. An IR illumination at 325°C for 100 s was inserted at the end of each SAR measurement cycle to reduce the effect of recuperation (based on Murray and Wintle, 2003). The

initial 1.2 s of the pIRIR₂₉₀ decay curve minus a background from the last 100 s were used for D_e determination. The same integration limits were used for the IRSL signal observed during the preceding IR stimulation at 50°C (hereafter called IR₅₀) for comparison with the pIRIR₂₉₀ data.

The laboratory fading rate, expressed in terms of the percentage decrease of signal intensity per decade of time (the g -value; Aitken, 1985) was measured using artificially irradiated aliquots. After D_e measurement and a final IR illumination at 325°C for 100 s, the same aliquots were given a dose of ~ 180 Gy and measured using the post-IR IRSL SAR protocol with varying storage times after irradiation and preheat (Auclair *et al.*, 2003). Storage times ranged from as short as experimentally possible ('prompt') to delays of ~ 10 hours. Fading rates for both IR₅₀ and pIRIR₂₉₀ were calculated following Equation 4 from Huntley and Lamothe (2001) using an excel macro (Huot, private communication, 2008).

To test whether doses given before any heating (i.e. as close as we can get to natural conditions) can be measured accurately, we carried out dose recovery tests. Six natural aliquots of selected samples (**Table 1**) were bleached for 4 hours in a Hönl SOL2 simulator (sample to lamp distance ~ 1.2 m to avoid heating of the aliquots). Three aliquots per sample were then given a beta dose similar to the measured D_e for each sample and the given dose measured using the above mentioned settings. Using the other bleached aliquots the equivalent doses after bleaching, i.e. residuals, were measured.

Table 1. Sample information, dose rates (taken from Watanuki *et al.*, 2005), recycling ratios, recuperation, measured to given dose ratios, and intercalated tephras for the loess section at Niigata (Tm) and Tochigi Prefecture (Tg).

Depth (m)	Sample ID	Tephra name ^a	Dose rate (Gy/ka) ^a	Number of aliquots	Recuperation (%)		Recycling ratio		Measured to given dose ratio	
					IR ₅₀	pIRIR ₂₉₀	IR ₅₀	pIRIR ₂₉₀	IR ₅₀	pIRIR ₂₉₀
Niigata										
0.40		AT								
1.10	Tm 2		1.35±0.09	6	6.3±1.9	1.9±0.5	0.88±0.06	1.00±0.02	0.85±0.15	1.01±0.06
1.40		DKP								
1.60	Tm 3		1.40±0.10	6	5.2±1.4	1.1±0.4	1.16±0.06	0.95±0.03		
2.10	Tm 4		1.36±0.09	6	6.2±1.8	2.4±0.6	1.08±0.04	1.00±0.04		
2.60	Tm 5		0.95±0.06	6	4.2±1.2	3.4±0.6	1.30±0.30	0.98±0.03		
2.80		Iz-KT								
3.10	Tm 6		1.22±0.10	4	4.9±2.2	1.0±0.2	1.00±0.03	1.00±0.01		
4.10	Tm 8		1.80±0.12	4	1.3±0.7	0.8±0.2	0.99±0.04	0.99±0.02	0.91±0.03	1.57±0.22
4.60	Tm 9		0.67±0.06	4	4.5±0.8	1.8±0.4	0.99±0.06	1.00±0.01		
5.10	Tm 10		0.94±0.08	4	4.7±1.7	0.9±0.3	0.97±0.07	0.98±0.01		
5.60	Tm 11		0.86±0.06	4	1.4±0.1	0.8±0.2	0.96±0.04	0.99±0.01		
6.10	Tm 12		0.80±0.06	4	2.4±1.0	1.0±0.2	0.98±0.04	0.98±0.01	1.08±0.10	1.27±0.07
9.00		APm								
Tochigi										
1.0	Tg 1		1.28±0.07	4	9.1±4.1	3.8±2.1	1.04±0.03	0.99±0.03	1.40±0.34	1.03±0.10
1.8	Tg 6		0.91±0.05	4	7.9±0.6	4.5±1.1	1.08±0.07	1.00±0.04		
2.0	Tg 7	Ag-KP	0.81±0.04	4	4.8±1.6	4.2±1.4	1.08±0.05	0.98±0.02		
4.1	Tg 10	Aso-4	0.85±0.05	4	3.5±1.8	2.7±0.5	1.11±0.05	0.96±0.02		
8.7	Tg 12	Iz-KT	0.72±0.04	4	13.8±4.4	2.5±1.1	1.06±0.07	1.05±0.05	1.57±0.45	1.22±0.09
9.6		APm-U								
10.1	Tg 15		0.94±0.06	4	4.3±2.1	0.7±0.1	0.94±0.04	1.02±0.05		
11.0		KdP								
20.9	Tg 16	Nm-13	0.93±0.05	4	6.6±2.5	0.8±0.1	1.05±0.08	1.00±0.01	0.85±0.10	1.39±0.20
22.4		Nm-14								
24.0		Nm-16								
35.4		HtB								
35.8	Tg 22		0.86±0.07	4	6.0±2.7	0.8±0.5	1.08±0.04	1.00±0.02	1.05±0.06	1.11±0.02

^a taken from Watanuki *et al.*, 2005.

4. MEASUREMENT PERFORMANCE AND FADING

Niigata

Laboratory dose response curves of one young (Tm 6) and one old (Tm 12) sample of the Niigata section are shown in Fig. 2. The dose responses of the IR₅₀ and pIRIR₂₉₀ signals are indistinguishable up to ~200 Gy; beyond that the growth curve for pIRIR₂₉₀ signal seems to flatten off earlier. For both samples the natural sensitivity corrected IR₅₀ signal is about 65% of the sensitivity corrected pIRIR₂₉₀ signal; this is representative of all samples from the Niigata section. The initial intensity of the pIRIR₂₉₀ signal is much larger than the rather weak IR₅₀ signal (although the latter is clearly above background; see insets Fig. 2). These observations agree well with former studies on post-IR IRSL dating (Buylaert *et al.*, 2009, Thiel *et al.*, 2011).

Recuperation of the IR₅₀ signal is <5% for most samples, ranging from 1.4±0.1% (Tm 11; n=4) to 6.3±1.9% (Tm 2; n=6) (Table 1). For the pIRIR₂₉₀ signal recuperation

varies between 0.8±0.2% (Tm 8; n=4) and 3.4±0.6% (Tm 5; n=6). There is no correlation between the recuperation of the IR₅₀ signal and that of the pIRIR₂₉₀ signal. Watanuki *et al.* (2005) observed similar recuperation when using IRSL at 50°C (detection in the UV), but found recuperation >10% in many of the quartz OSL measurements. Recycling ratios for both signals and all samples are within 10% of unity. The results of dose recovery tests, which were conducted for three samples of the Niigata section (Table 1), varied considerably among different samples (Fig. 3). The mean measured to given ratios after subtraction of a residual signal (pIRIR₂₉₀ 20±2 Gy (n=9), IR₅₀ 5±1 Gy (n=9)) are 1.28±0.12 (n=9) for pIRIR₂₉₀ and 0.95±0.09 (n=9) for IR₅₀, respectively. We speculate that the large residuals and the not very satisfactory dose recovery results might suggest that the bleaching in the SOL2 simulator is not representative of bleaching in nature. The measured fading rates for pIRIR₂₉₀ vary between 0.04±1.17 %/decade (n=3) and 1.94±1.43 %/decade (n=3); negative g-values were derived for IR₅₀ (Table 2) which may indicate some form of recuperation with storage. We do not have an explanation

for this increase of the IR_{50} signal intensity with time. This clearly needs further investigations but lies out of the scope of this dating study (which is focused on the applicability of the pIRIR_{290} signal).

Tochigi

Most samples from the Tochigi section show characteristics (Fig. 4) and SAR performance (Table 1) similar to Niigata section. The dose response curves of IR_{50} and pIRIR_{290} for sample Tg 6 (representative of samples Tg 1 to Tg 10) are identical up to 300 Gy (Fig. 4a), whereas for sample Tg 22, representing samples Tg 12 to Tg 22, the curves are indistinguishable up to ~150 Gy with a steeper growth for the IR_{50} at larger doses (Fig. 4b). For the young samples (Tg 1 to Tg 6) the sensitivity corrected natural pIRIR_{290} is smaller than that of IR_{50} (Fig. 4a; see also equivalent doses in Table 2), whereas for the older samples the opposite is true; this difference is very pronounced for the oldest sample (Tg 22; Fig. 4b).

For the IR_{50} signal recuperation for only three samples is <5% (Tg 7, Tg 10 and Tg 15; Table 1); the values vary

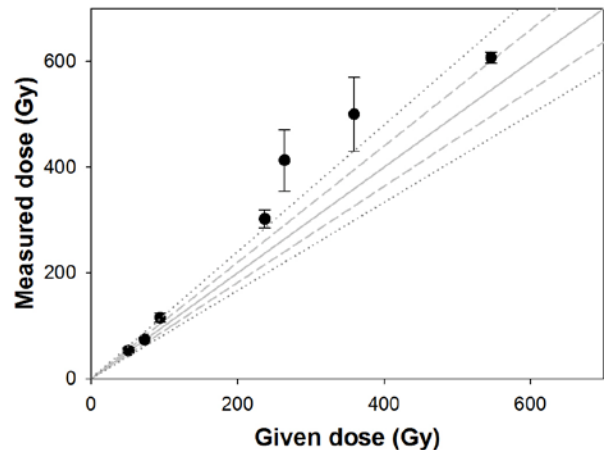


Fig. 3. Measured doses plotted against given doses of pIRIR_{290} for all samples from Niigata and Tochigi. The errors shown are 1 σ . Dose recovery results for IR_{50} are not shown, because the focus of this study is the pIRIR_{290} signal. For completeness, the dose recovery results of IR_{50} are presented in section 4. The dashed lines indicate $\pm 10\%$ around unity and the dotted lines $\pm 20\%$, respectively.

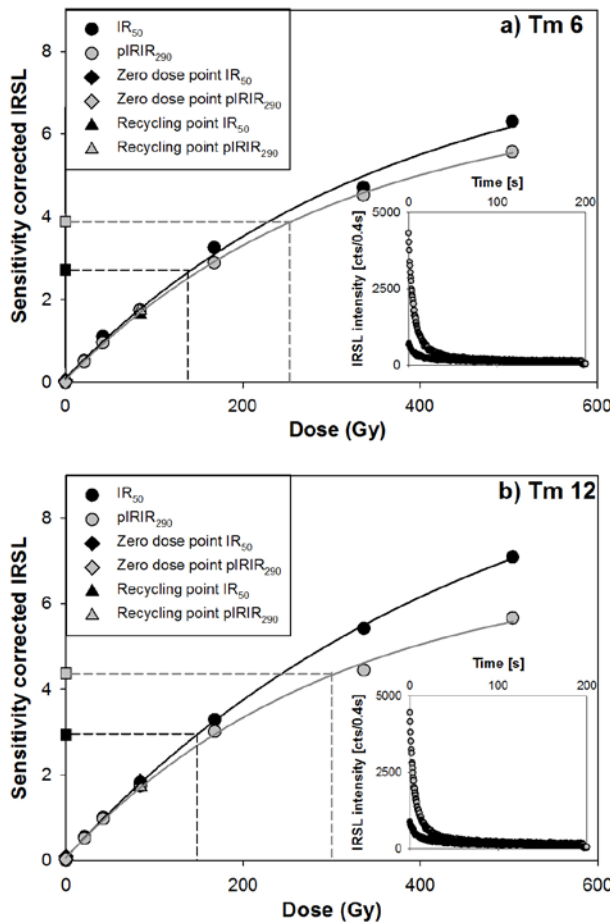


Fig. 2. Dose response and natural decay curves (inset) for samples Tm 6 (a) and Tm 12 (b); the latter represents the oldest sample at the section in Niigata Prefecture.

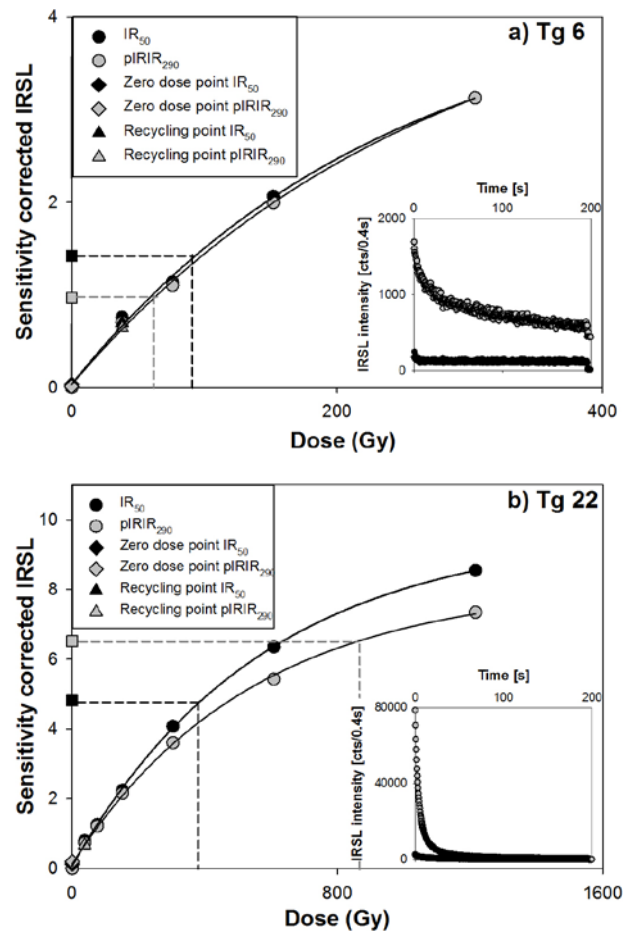


Fig. 4. Dose response and natural decay curves (inset) for samples Tg 6 (a) and Tg 22 (b); the latter represents the oldest sample at the section in Tochigi Prefecture.

between $3.5 \pm 1.8\%$ (Tg 10; n=4) and $13.8 \pm 4.4\%$ (Tg 12; n=4) and are significantly larger than for Niigata section. Recuperation for the pIRIR₂₉₀ signal is smaller and ranges from $0.7 \pm 0.1\%$ (Tg 15; n=4) to $4.5 \pm 1.1\%$ (Tg 6; n=4). The dose recovery test results are similar to the Niigata section (**Table 1**; **Fig. 3**). After subtraction of a residual (pIRIR₂₉₀ 15 ± 2 Gy, IR₅₀ 3 ± 1 Gy) the mean measured to given dose ratios are 1.19 ± 0.10 (n=9) for pIRIR₂₉₀ and 1.22 ± 0.24 (n=9) for IR₅₀.

The laboratory fading rates range from $0.07 \pm 0.78\%$ /decade (n=3) to $2.00 \pm 0.64\%$ /decade (n=3). For IR₅₀ negative values were again observed (**Table 2**). Watanuki *et al.* (2005) also found an IRSL signal increase (measured in the UV) of $\sim 280\%$ for the sample which they measured after storage at 100°C for two weeks; this is hence in accordance with our observations.

Does the pIRIR₂₉₀ signal show significant fading?

The distributions of the fading rates for both IRSL signals from both sites are shown in **Fig. 5**. The measured negative fading rates for IR₅₀ (in the following referred to as ‘apparent fading rate’; **Table 2**) are presumably not representative of what is occurring in nature. The measured fading rates for pIRIR₂₉₀ are on average close to 1.0 (**Fig. 5b**), but due to the unreliability of the IR₅₀ fading rates it is difficult to judge whether the measured fading rates for pIRIR₂₉₀ represent the natural fading rates. This emphasises the need for IRSL dating procedures that are

not reliant on fading corrections. It has been suggested that the post-IR IRSL signal measured at 290°C does not fade significantly (Thiel *et al.* 2011), based on the observation of a natural signal in saturation on a laboratory dose response curve for a sample from below B/M boundary. The observations of Thiel *et al.* (2011) were made on polymimetic fine grains extracted from European loess; the luminescence characteristics and fading behaviour are however not identical to the sites under study. There is no Japanese loess old enough to be in saturation. We refer to the work of Buylaert *et al.* (2011) in which they investigated the saturation behaviour of the pIRIR₂₉₀ signal from a Chinese loess sample (Luochuan section) from well below B/M boundary. If indeed Japanese loess is a mixture of Chinese loess, air-fall tephra and local dust (Suzuki, 1995) then this sample should be at least partly representative of our material.

Fig. 6 shows the dose response curve for the polymimetic fine grain extracts from China with the natural of the IR₅₀ signal and the pIRIR₂₉₀ signal interpolated on the curves. The L_x/T_x values were normalised using the saturation value. It is evident that the natural for the pIRIR₂₉₀ signal is in, or close to saturation, whereas the natural for the IR₅₀ signal is less than 60% of the laboratory saturation level. From that we conclude that it is unlikely that any fading correction is needed when making use of pIRIR₂₉₀; the following discussion thus concentrates on the uncorrected pIRIR₂₉₀ signal, and all ages are presented without the subtraction of a residual.

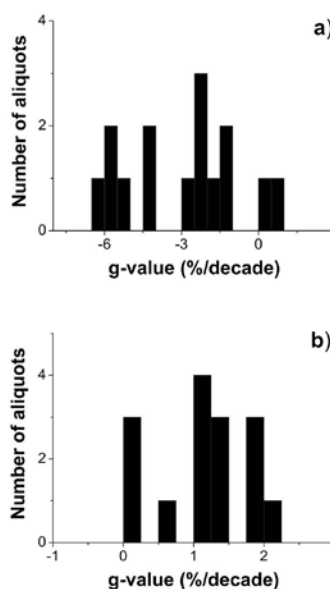


Fig. 5. Histograms of g-values measured for a) IR₅₀ and b) pIRIR₂₉₀, showing that for pIRIR₂₉₀ the g-values scatter around 1.0%/decade.

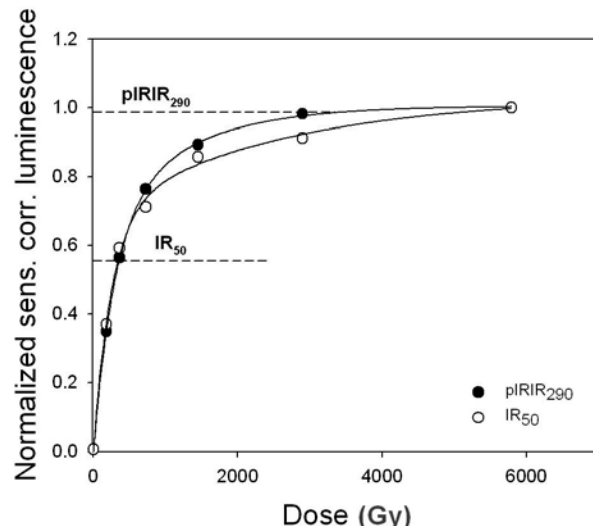


Fig. 6. Dose response curves for a Chinese loess sample from well below Brunhes/Matuyama boundary. The expected dose is $\sim 3\text{kGy}$. The dashed lines show the natural of IR₅₀ and pIRIR₂₉₀, respectively. (modified from Buylaert *et al.*, 2011)

5. COMPARISON WITH INDEPENDENT AGE CONTROL

Niigata section

At the Niigata section the uncorrected pIRIR₂₉₀ ages, apart from two outliers (Tm 8 and Tm 10; **Table 2**), increase with depth (**Fig. 7**) and follow the trend of the tephra ages. For comparison, the fading uncorrected IR₅₀ ages are also plotted in **Fig. 7**; these clearly show field saturation at ~150 ka (in this context, field saturation is the condition where the rate of charge trapping is equal to the rate of charge loss). It should be remembered that fading correction of the IR₅₀ ages would not improve this comparison because: (i) the apparent fading rates are negative; (ii) once in field saturation any chronological information is lost; and (iii) there are no proven fading

correction methods that can be applied beyond the linear region of the growth curve. The two outliers in pIRIR₂₉₀ age follow the trend of the quartz ages, in that the ages are younger than those of the overlying samples (**Table 2**); this suggests a problem with the dose rate estimation rather than a dose measurement problem because the measured water content for these samples were over 100%. Overall there is good agreement with the quartz ages presented in Watanuki *et al.* (2005). This can be seen in **Fig. 8**, where the pIRIR₂₉₀ ages are plotted against the quartz OSL ages (a comparison with tephra ages is not shown here because they do not originate from the same depths). The pIRIR₂₉₀ tend to overestimate the quartz ages for the younger sample by 5–10%; this overestimate rapidly decreases for the older samples, and is negligible >150 ka. Sample Tm 12 (pIRIR₂₉₀: 291±33 ka)

Table 2. Equivalent doses, g-values, fading uncorrected and fading corrected ages for Niigata (Tm) and Tochigi (Tg). For comparison quartz OSL and tephra ages taken from Watanuki *et al.* (2005) are listed.

Depth (m)	Sample ID	Equivalent dose (Gy)		g-value (%/decade)		fading uncorrected age (ka)		fading corrected age (ka)		Tephra age (ka) ^c	Quartz OSL age (ka) ^d
		IR ₅₀	pIRIR ₂₉₀	IR ₅₀	pIRIR ₂₉₀	IR ₅₀	pIRIR ₂₉₀	IR ₅₀	pIRIR ₂₉₀		
Niigata											
0.40										26-29	
1.10	Tm 2	48±5	86±3	-4.50±1.19	1.11±1.00	35±4	64±2	n.a. ^a	70±9		56±4
1.40										≥ 55	
1.60	Tm 3	99±5	143±7	-2.04±1.26	1.04±0.89	71±4	102±5	n.a. ^a	112±14		81±6
2.10	Tm 4	95±12	160±4	-2.31±1.27	1.41±1.07	70±9	118±3	n.a. ^a	134±17		99±7
2.60	Tm 5	112±17	161±9	n.a.	n.a.	118±18	170±10	n.a.	n.a.		145±14
2.80										125-150	
3.10	Tm 6	157±25	284±30	-1.22±1.25	1.82±1.09	128±22	233±26	n.a. ^a	276±49		155±19 ^e
4.10	Tm 8	155±15	298±27	0.32±1.73	1.76±1.13	86±9	166±16	89±14 ^b	195±32		156±12
4.60	Tm 9	93±5	175±8	-1.81±2.31	0.12±1.34	138±9	261±14	n.a. ^a	264±33		203±21 ^e
5.10	Tm 10	115±4	205±13	n.a.	n.a.	122±5	218±16	n.a.	n.a.		199±18
5.60	Tm 11	124±8	270±23	-4.39±2.01	0.04±1.17	144±10	314±28	n.a. ^a	315±39		298±23
6.10	Tm 12	111±12	233±25	0.91±2.01	1.94±1.43	139±16	291±33	151±31 ^b	351±72		228±20
9.00										330-400	
Tochigi											
1.0	Tg 1	109±25	67±3			85±9	52±7				36±3 ^e
1.8	Tg 6	88±7	59±7	-6.03±1.38	1.02±0.91	97±6	65±5	n.a. ^a	71±11		
2.0	Tg 7	72±10	53±4	-5.07±1.73	0.07±0.78	89±6	65±4	n.a. ^a	59±6	≥ 45	
4.1	Tg 10	68±11	118±14	-5.96±1.71	1.09±0.16	80±14	139±18	n.a. ^a	154±18	85-90	94±10
8.7	Tg 12	40±6	101±2	-5.52±2.24	2.00±0.64	56±4	141±8	n.a. ^a	170±16	125-150	
9.6										130±30	150±15
10.1	Tg 15	90±3	227±25	-2.34±1.63	1.47±0.24	95±6	241±18	n.a. ^a	277±36		209±14
11.0										200±30	
20.9	Tg 16	97±30	384±87	-1.47±1.73	1.45±0.31	104±16	413±43	n.a. ^a	474±111	330-400	303±20
22.4										330-400	
24.0										330-400	
35.4										660±40	
35.8	Tg 22	204±52	528±33	-2.91±1.81	0.74±0.15	237±35	614±52	n.a. ^a	658±68		507±41

^a Fading correction could not be applied due to negative g-values.

^b Fading correction is using the measured g-value, which is assumed to be not representative for what is occurring in nature. For details see text.

^c Tephra ages taken from Watanuki *et al.*, 2005. For more details on the tephra ages see text.

^d Quartz OSL ages taken from Watanuki *et al.*, 2005. Unless otherwise indicated the OSL ages are Component-1 quartz blue-OSL, which has been considered the most reliable age estimate.

^e Component-1 polymimetal blue-OSL age; no Component-1 quartz blue-OSL age available.

seems to overestimate the relevant quartz OSL age (228 ± 20 ka), but compared to the pIRIR₂₉₀ and OSL ages of the overlying sample (Tm 11), it is more likely that the quartz OSL age of Tm 12 is an underestimate (Table 2).

Tochigi section

The observations for Tochigi section are similar to the Niigata section. The uncorrected pIRIR₂₉₀ ages are plotted against depth in Fig. 9; for comparison the fading uncorrected IR₅₀ ages are shown. The uppermost samples show surprising behaviour, with fading uncorrected IR₅₀ ages older than pIRIR₂₉₀ ages (Table 2). As at Niigata, a

small overestimation of the tephra age for the younger samples is seen, but the pIRIR₂₉₀ ages clearly result in more reliable age estimates than the IR₅₀ signal; for the older samples (>200 ka) there is good agreement with the tephra ages. This is also shown in Fig. 10, which also includes a comparison with quartz OSL ages. Apart from sample Tg 10, for which the pIRIR₂₉₀ age is an overestimate of ~ 25 ka compared to the tephra and quartz OSL ages (Table 2), there is a good agreement of pIRIR₂₉₀ and tephra ages. Compared to quartz OSL, the pIRIR₂₉₀ results seem to overestimate for the older samples (Fig. 10; Table 2); however, Watanuki *et al.* (2005) found that for

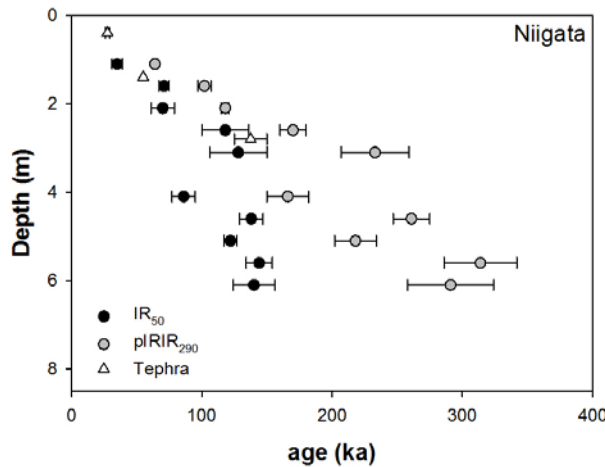


Fig. 7. Fading uncorrected IR₅₀ ages (black circles), uncorrected pIRIR₂₉₀ ages (grey circles) and tephra ages (open triangles) of Niigata plotted against depth. The IR₅₀ ages saturate at about 150 ka, whereas the pIRIR₂₉₀ ages increase with depth (apart from two outliers; for details see text). The errors are given as 1σ .

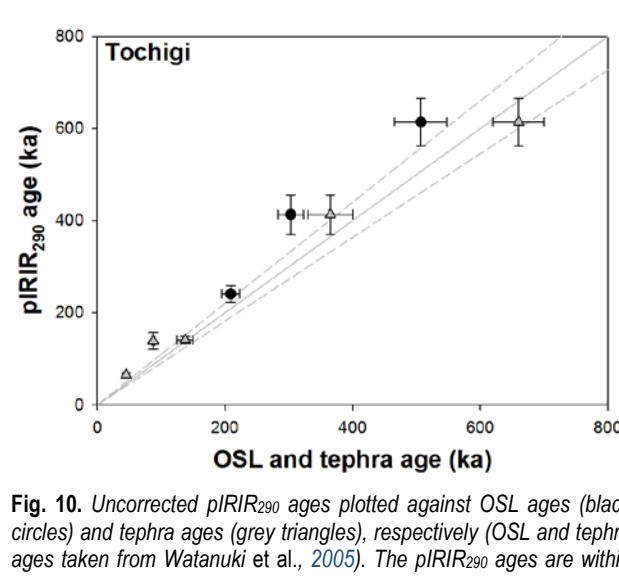
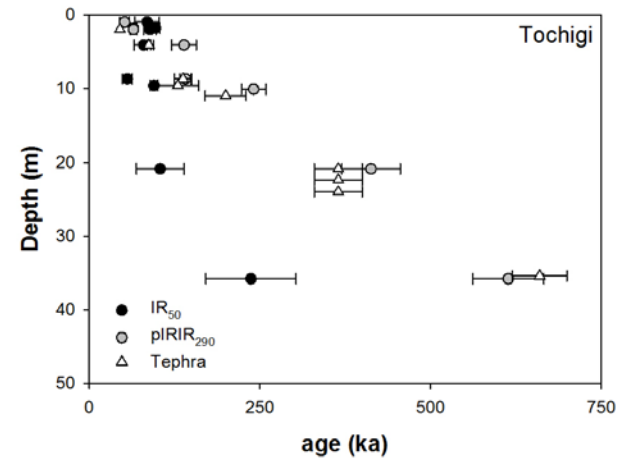


Fig. 10. Uncorrected pIRIR₂₉₀ ages plotted against OSL ages (black circles) and tephra ages (grey triangles), respectively (OSL and tephra ages taken from Watanuki *et al.*, 2005). The pIRIR₂₉₀ ages are within errors (1σ) in reasonable agreement with the tephra ages for most of the samples, whereas they tend to overestimate the OSL ages (dashed lines show $\pm 10\%$ around unity). For discussion see text.

Fig. 8. Fading uncorrected pIRIR₂₉₀ ages plotted against OSL ages (taken from Watanuki *et al.*, 2005). The errors shown are 1σ . Compared to the OSL ages, the pIRIR₂₉₀ ages tend to overestimate up to 10% (dashed lines show $\pm 10\%$ around unity).

the older samples the quartz OSL ages tend to slightly underestimate the tephra ages. We conclude that the pIRIR₂₉₀ ages can be considered at least as reliable as the quartz OSL ages.

At both sites there is a tendency for the pIRIR₂₉₀ to slightly overestimate the quartz ages (**Table 2; Figs. 8 and 10**). For the younger ages this is likely to arise from the residual doses observed (but not subtracted, cf. Thiel *et al.*, 2011). For older material, the residual is not significant; in this age range we consider it more likely that the quartz ages underestimate the true ages. Watanuki *et al.* (2005) concluded that the quartz D_e values are likely to be saturated although the dose response curve still grows, and so the pIRIR₂₉₀ ages are more likely to be correct. This conclusion is supported by the good agreement between the pIRIR₂₉₀ and tephra ages for the lowest level at the Tochigi site.

6. CONCLUSIONS

We have tested an elevated temperature post-IR IRSL dating protocol on two Japanese loess sections for which quartz OSL and tephra ages are also available. The elevated temperature post-IR IRSL signal was measured at 290°C after a preheat of 320°C (60 s) and an IR bleach at 50°C. The applicability of our SAR protocol was tested by examining the standard criteria, i.e. recycling ratios, recuperation, and measured to given dose ratios in dose recovery experiments. Recuperation of the pIRIR₂₉₀ signal is <5% for all samples and all recycling ratios are close to unity. Dose recovery results are less satisfactory, and are both around two standard errors greater than unity. Nevertheless, it is evident from the comparison with the independent age control that our SAR post-IR IRSL dating results in ages that are at least as accurate as quartz, and possibly more so. These data are not corrected for fading, and this decision is supported by the natural pIRIR₂₉₀ signal lying in the saturated region of the laboratory growth curve in a loess sample from an upwind Chinese site.

We present this study as a step towards more reliable feldspar luminescence dating. Our data show that post-IR IRSL dating is applicable to polymimetic fine grains extracted from Japanese loess. Future work needs to focus on a better understanding of the physical processes involved in post-IR IRSL dating, an explanation of the unsatisfactory dose recovery experiments, and more appropriate measurements protocols applicable to different environments.

ACKNOWLEDGEMENTS

This paper is dedicated to the memory of Takuya Watanuki. CT and ST have been supported by the Leibniz Pakt for Research and Innovation 2008-10. We are grateful to Mayank Jain and Kristina Thomsen for fruitful discussions on post-IR IRSL dating. We appreciate the

reviewers' comments on an earlier version of this manuscript.

REFERENCES

- Aitken MJ, 1985. *Thermoluminescence Dating*. London, Academic Press: 359pp.
- Auclair M, Lamothe M and Hout S, 2003. Measurement of anomalous fading for feldspar IRSL using SAR. *Radiation Measurement* 37(4-5): 487-492, DOI [10.1016/S1350-4487\(03\)00018-0](https://doi.org/10.1016/S1350-4487(03)00018-0).
- Buylaert JP, Murray AS, Thomsen KJ and Jain M, 2009. Testing the potential of an elevated temperature IRSL signal from K-feldspar. *Radiation Measurements* 44(5-6): 560-565, DOI [10.1016/j.radmeas.2009.02.007](https://doi.org/10.1016/j.radmeas.2009.02.007).
- Buylaert JP, Thiel C, Murray AS, Vandenberghe DAG, Yi S, Lu H, 2011. IRSL and post-IR IRSL residual doses recorded in modern dust samples from the Chinese Loess Plateau. *Geochronometria* 38(4): 432-440, DOI [10.2478/s13386-011-0047-0](https://doi.org/10.2478/s13386-011-0047-0).
- Frechen M, Horváth E and Gábris G, 1997. Geochronology of Middle to Upper Pleistocene Loess Sections in Hungary. *Quaternary Research* 48(3): 291-312, DOI [10.1006/qres.1997.1929](https://doi.org/10.1006/qres.1997.1929).
- Hayatsu K and Arai F, 1981. Tephrochronological study on the Shinanogawa tephra formations at the middle course of the Sinano River, central Japan. *Journal of Geography (Chigaku-zasshi)* 91: 88-103 (in Japanese with English abstract).
- Huntley DJ and Lamothe M, 2001. Ubiquity of anomalous fading in K-feldspars and the measurement and correction for it in optical dating. *Canadian Journal of Earth Science* 38(7): 1093-1106, DOI [10.1139/e01-013](https://doi.org/10.1139/e01-013).
- Kaizuka S, Koike K, Endo K, Yamazaki H and Suzuki T, 2000. *Regional Geomorphology of the Japanese Islands. Vol. 4: Geomorphology of Kanto and Izu-Ogasawara*. University of Tokyo Press: 349pp. (in Japanese).
- Kars RH, Wallinga J and Cohen KM, 2008. A new approach towards anomalous fading correction for feldspar IRSL dating - tests on samples in field saturation. *Radiation Measurements* 43(2-6): 786-790, DOI [10.1016/j.radmeas.2008.01.021](https://doi.org/10.1016/j.radmeas.2008.01.021).
- Lamothe M and Auclair M, 1999. A solution to anomalous fading and age shortfalls in optical dating of feldspar minerals. *Earth and Planetary Science Letters* 171(3): 319-323, DOI [10.1016/S0012-821X\(99\)00180-6](https://doi.org/10.1016/S0012-821X(99)00180-6).
- Lamothe M, Auclair M, Hamzaoui C and Huot, S, 2003. Towards a prediction of long-term anomalous fading of feldspar IRSL. *Radiation Measurements* 37(4-5): 493-498, DOI [10.1016/S1350-4487\(03\)00016-7](https://doi.org/10.1016/S1350-4487(03)00016-7).
- Machida H and Arai F, 2003. *Atlas of Tephra in and around Japan*. University of Tokyo Press: 337pp. (in Japanese).
- Miyairi Y, Yoshida K, Miyazaki Y, Matsuzaki H and Kaneoka I, 2004. Improved ¹⁴C dating of tephra layer (AT tephra, Japan) using AMS on selected organic fractions. *Nuclear Instruments and Methods in Physics Research Section B: Beam Interactions with Materials and Atoms* 223-224: 555-559, DOI [10.1016/j.nimb.2004.04.103](https://doi.org/10.1016/j.nimb.2004.04.103).
- Morthekai P, Jain M, Murray AS, Thomsen KJ and Bøtter-Jensen L, 2008. Fading characteristics of martian analogue materials and the applicability of a correction procedure. *Radiation Measurements* 43(2-6): 672-678, DOI [10.1016/j.radmeas.2008.02.019](https://doi.org/10.1016/j.radmeas.2008.02.019).
- Murray AS and Wintle AG, 2003. The single aliquot regenerative dose protocol: potential for improvements in reliability. *Radiation Measurements* 37(4-5): 377-381, DOI [10.1016/S1350-4487\(03\)00053-2](https://doi.org/10.1016/S1350-4487(03)00053-2).
- Murray AS, Buylaert JP, Thomsen KJ and Jain M, 2009. The Effect of Preheating on the IRSL Signal from Feldspar. *Radiation Measurements* 44(5-6): 554-559, DOI [10.1016/j.radmeas.2009.02.004](https://doi.org/10.1016/j.radmeas.2009.02.004).
- Novothny Á, Horváth E and Frechen M, 2002. The loess profile of Albertirska, Hungary - Improvements in loess stratigraphy by luminescence dating. *Quaternary International* 95-96: 155-163, DOI [10.1016/S1040-6182\(02\)00036-8](https://doi.org/10.1016/S1040-6182(02)00036-8).
- Spooner NA, 1994. The anomalous fading of infrared-stimulated luminescence from feldspars. *Radiation Measurements* 23(2-3): 625-632, DOI [10.1016/1350-4487\(94\)90111-2](https://doi.org/10.1016/1350-4487(94)90111-2).

- Suzuki T, 1995. Origin of so-called volcanic ash soil: thickness distribution in and around central Japan. *Bulletin of the Volcanological Society of Japan* 40: 167-176 (in Japanese with English abstract).
- Suzuki T, 2001. Iizuna-Kamitaru tephra group erupted from the Iizuna volcano of Myoko volcano group in the transition from isotope stage 6 to 5, and its significance for the chronological study of central Japan. *Quaternary Research (Daiyonki-kenkyu)* 40: 29-41 (in Japanese with English abstract).
- Suzuki T, Fujiwara T and Danhara T, 1998. Fission track ages of eleven Quaternary tephras in north Kanto and south Tohoku regions, central Japan. *Quaternary Research (Daiyonki-kenkyu)* 37: 95-106 (in Japanese with English abstract).
- Thiel C, Buylaert JP, Murray AS, Terhorst B, Hofer I, Tsukamoto S and Frechen M, 2011. Luminescence dating of the Stratzing loess profile (Austria) - Testing the potential of an elevated temperature post-IR IRSL protocol. *Quaternary International* 234(1-2): 23-31, DOI: [10.1016/j.quaint.2010.05.018](https://doi.org/10.1016/j.quaint.2010.05.018).
- Thomsen KJ, Bøtter-Jensen L, Denby PM, Moska P and Murray AS, 2006. Developments in luminescence measurement techniques. *Radiation Measurements* 41(7-8): 768-773, DOI [10.1016/j.radmeas.2006.06.010](https://doi.org/10.1016/j.radmeas.2006.06.010).
- Thomsen KJ, Murray AS, Jain M and Bøtter-Jensen L, 2008. Laboratory fading rates of various luminescence signals from feldspar-rich sediment extracts. *Radiation Measurements* 43(9-10): 1474-1486, DOI [10.1016/j.radmeas.2008.06.002](https://doi.org/10.1016/j.radmeas.2008.06.002).
- Tsukamoto S, Murray A, Huot S, Watanuki T, Denby PM and Bøtter-Jensen L, 2007. Luminescence property of volcanic quartz and the use of red isothermal TL for dating tephras. *Radiation Measurements* 42(2): 190-197, DOI [10.1016/j.radmeas.2006.07.008](https://doi.org/10.1016/j.radmeas.2006.07.008).
- Watanuki T, Murray AS and Tsukamoto S, 2005. Quartz and poly-mineral luminescence dating of Japanese loess over the last 0.6 Ma: Comparison with an independent chronology. *Earth and Planetary Science Letters* 240(3-4): 774-789, DOI [10.1016/j.epsl.2005.09.027](https://doi.org/10.1016/j.epsl.2005.09.027).
- Wintle AG, 1973. Anomalous Fading of Thermoluminescence in Minerals. *Nature* 245(5421): 143-144, DOI [10.1038/245143a0](https://doi.org/10.1038/245143a0).